






## Article

# Development of a Process to Recycle NdFeB Permanent Magnets Based on the CaO-Al<sub>2</sub>O<sub>3</sub>-Nd<sub>2</sub>O<sub>3</sub> Slag System

Ludwig W. Blenau <sup>1,\*</sup> , Daniel Vogt <sup>1</sup> , Oliver Lonski <sup>1</sup> , Abuzar Abrar <sup>1</sup> , Olga Fabrichnaya <sup>2</sup>   
and Alexandros Charitos <sup>1</sup> 

<sup>1</sup> Institute for Nonferrous Metallurgy and Purest Materials (INEMET), TU Bergakademie Freiberg, Leipziger Str. 34, D-09599 Freiberg, Germany; daniel.vogt@inemet.tu-freiberg.de (D.V.); oliver.lonski@tuhh.de (O.L.); abuzarabrar92@gmail.com (A.A.); alexandros.charitos@inemet.tu-freiberg.de (A.C.)

<sup>2</sup> Institute of Materials Science, TU Bergakademie Freiberg, Gustav-Zeuner-Str. 5, D-09599 Freiberg, Germany; fabrich@ww.tu-freiberg.de

\* Correspondence: ludwig.blenau@inemet.tu-freiberg.de; Tel.: +49-03731-392051

**Abstract:** Nd, Pr and Dy are critical raw materials as major components for rare earth permanent magnets (REPM). These are integral for several components placed for example within electric vehicles and wind turbine generators. REE primary production is mainly realized in China (~80%) and no REPM recycling industry has been established. Hydrometallurgical recycling routes lead to iron dissolution (66 wt. % Fe in REPM), while pyrometallurgical approaches that utilize SiO<sub>2</sub> risk contaminating the produced iron phase. A two-step process is presented that (i) creates an FeO<sub>x</sub>-CaO-Al<sub>2</sub>O<sub>3</sub>-REE<sub>2</sub>O<sub>3</sub> molten slag at 1500 °C through oxidative smelting and (ii) separates an iron-depleted slag phase (CaO-Al<sub>2</sub>O<sub>3</sub>-REE<sub>2</sub>O<sub>3</sub>) and a molten iron phase via carbothermic or metallothermic reduction at 1700–2000 °C. The slag has been designed as a selective collector phase and the REE<sub>2</sub>O<sub>3</sub> loading within the bulk slag can reach up to 25 wt. % REE<sub>2</sub>O<sub>3</sub> at 1700 °C. The contained minerals within the slag exhibit >40 wt. % REE (a higher REE concentration than in the initial REPM). The resulting phases are characterized via ICP-OES, CS and SEM-EDX. In addition, the first results with regard to the downstream hydrometallurgical processing of the CaO-Al<sub>2</sub>O<sub>3</sub>-REE<sub>2</sub>O<sub>3</sub> slag are presented aiming at the recovery of REE<sub>2</sub>O<sub>3</sub>, as well as of CaO and Al<sub>2</sub>O<sub>3</sub>. The latter compounds are to be reused during the first process step, i.e., the oxidative smelting of REPM. Slag leaching with methane sulfonic acid (MSA) and separation with alternative methods, such as solvent extraction, seems promising. Future work will include slag filtration with the aim to separate REE-rich solid phases (minerals) from the slag and also molten salt electrolysis of the produced REE<sub>2</sub>O<sub>3</sub> oxides.

**Keywords:** REPM recycling; neodymium recycling; pyrometallurgical magnet recycling; slag system design; Nd-rich minerals; CALPHAD; thermo-calc



**Citation:** Blenau, L.W.; Vogt, D.; Lonski, O.; Abrar, A.; Fabrichnaya, O.; Charitos, A. Development of a Process to Recycle NdFeB Permanent Magnets Based on the CaO-Al<sub>2</sub>O<sub>3</sub>-Nd<sub>2</sub>O<sub>3</sub> Slag System. *Processes* **2023**, *11*, 1783. <https://doi.org/10.3390/pr11061783>

Academic Editors: Mansoor Barati, Sina Mostaghel and Elmira Moosavi-Khoonsari

Received: 29 April 2023

Revised: 24 May 2023

Accepted: 6 June 2023

Published: 11 June 2023



**Copyright:** © 2023 by the authors. Licensee MDPI, Basel, Switzerland. This article is an open access article distributed under the terms and conditions of the Creative Commons Attribution (CC BY) license (<https://creativecommons.org/licenses/by/4.0/>).

## 1. Introduction

Rare earth elements (REEs) such as Nd, Pr and Dy are essential for rare earth permanent magnets (REPM) which in turn are used in all kinds of electric motors, generators and other devices. REPMs account for ca. one quarter of the total REE demand [1], 76% of the Nd and 70% of the Pr demand, respectively [2]. Since 80% of the production is carried out in the People's Republic of China (PRC) and 20% in Japan or the European Union (EU) [3], Nd is listed in all four lists of "critical raw materials" by the EU [4].

The main sources for REPM recycling are large magnets, and production residues [1], while small REPM in, for example, consumer electronics are usually not separated. While small consumer electronics need only around 1 g of magnets, electric vehicles need about 1 kg and modern windmills contain magnets in the 1–2 t range [2]. Since the magnets are based on the Nd<sub>2</sub>Fe<sub>14</sub>B composition, they contain typically 31–32 wt. % of REEs, because REEs are typically overstoichiometric [5]. The main body of the magnets contains roughly 23–31 wt. % Nd, 0–7 wt. % Pr, 1.3–5 wt. % of Dy, 65–70 wt. % of Fe, 0.9–1.2 wt. % of B and

0–2 wt. % of La. The coating (responsible for corrosion resistance) contains, for example, Co, Al, Ni and Nb while typical contaminants are C, Ca, N, Si and O. Another source is Hard Disk Drives (HDDs) from waste electronics accounting for 6000–12,000 t of Nd-Fe-B alloys annually [6].

When considering the recycling of REPM, three main approaches can be discussed: (i) the reuse of (typically larger) end-of-life magnets in new products; (ii) direct recycling of the end-of-life REPMs via remelting into a new master alloy (direct pyrometallurgical recycling, termed also as the short recycling route) and (iii) the production of pure REE-oxides from the REPMs, which in turn can be used to produce new REPMs (termed also as the long recycling route) [6,7]. The focus of this work is on approach (iii), since approaches (i) and (ii) are only feasible for certain types and purities of magnets. On the other hand, approach (iii) can incorporate all kinds of waste streams such as manufacturing swarfs and exhibits more tolerance to contamination. In addition, the direct remelting of magnets into a new REPM master alloy—i.e., approach (ii)—still proves challenging, because REPMs are produced through a sintering process in a magnetic field with fine-grained pure elements [2,7].

The production of REE oxides from magnets can be realized through purely hydrometallurgical methods, as proven in fundamental studies [7,8]. There is however also initial research in utilizing pyrometallurgical processes to aid REPM recycling by separating the REE as oxides from Fe. Some not exhaustive examples are: Nakamoto et al. (2011) [9] successfully separated Fe in a metal phase from a REE oxide-rich phase using  $B_2O_3$  as flux at 1550 °C in graphite crucibles under an Ar atmosphere. Elwert et al. (2014) [10] used a  $Al_2O_3$ -CaO-MgO- $P_2O_5$ - $SiO_2$  slag system to concentrate up to 57 wt. % of REE oxides in the slag phase at 1500–1600 °C. Bian et al. (2015) [11] used REPM fragments, roasted at 1000 °C and subsequently produced a Fe-B metal phase and a 95 wt. % pure REE oxide phase through carbothermic reduction at 1550 °C. Kruse et al. (2015) [12] separated an Fe phase and a 90 wt. % pure REE oxide phase from REPM production sludges at 1550 °C in graphite crucibles, while utilizing  $B_2O_3$  as flux. Le et al. (2016) [13] worked with a  $Nd_2O_3$ -CaO- $SiO_2$  slag system at 1600 °C, producing Nd-rich mineral phases, that could be relevant for recycling. Borra et al. (2016) [14] produced a REE rich phase from red mud at 1500 °C utilizing  $CaSiO_3$  as flux and proposed the selective leaching of a REE oxide slag after removing Fe. Orefice et al. (2019) [15] performed carbothermic reduction at 1600 °C utilizing only  $CaCO_3$  as flux, which lead to a phase separation but not to a completely molten system. In general, while phase separation in the crucible scale works decently as soon as a liquid Fe phase is formed, for any kind of large-scale industrial process a more or less completely molten slag metal system is considered as highly beneficial.

While there is no commercial operation for End of Life (EoL) REPM today, it is estimated that recycling will play a significant role within a timescale of around 10 years [2]. In that sense, it is the authors' opinion that a pyrometallurgical step prior to hydrometallurgical treatment, in which the Fe (~66 wt. % of the REPM) is separated together with other contaminating metals (e.g., Ni, Co from the coating, Cu from WEEE parts or Ag, Au from e.g., HDDs) as a metal phase and the REEs are transferred to a REE-rich oxidic slag phase, can be advantageous. This should hold true considering that  $H_2$  evolution, occurring during direct magnet leaching [16], is avoided ( $Nd^{+3}$  is present during slag leaching). Moreover, the purity of the REE oxides is not influenced by the iron, as in the case of direct leaching [17]. Furthermore, considering the reuse of fluxing agents in the current approach, it may be stated that the generation of waste and the use of chemicals will be also less than direct leaching. In addition, the benefit of any pyrometallurgical process involving the slagging of metallic REE, as in the case of this work, is the heat generated by the autothermic REE oxidation which minimizes the amount of heat addition required. Closed system modelling, realized by the authors with use of HSC Chemistry commercial software [18], indicates that when fluxing magnet material at a ratio of 1:2.5, the desired process temperature can be reached even if no energy is transferred to the system.

## 2. Materials and Methods

Since REE oxides have high melting temperatures (2233 °C for Nd<sub>2</sub>O<sub>3</sub>), a liquid slag metal separation requires fluxing. The CaO-Al<sub>2</sub>O<sub>3</sub>-REE<sub>2</sub>O<sub>3</sub> system was chosen as a collector phase because it is a simple ternary system. In addition, CaO (available as CaCO<sub>3</sub>) as well as Al<sub>2</sub>O<sub>3</sub> are relatively cheap fluxing agents, readily available, nontoxic and presumably not interfering with regard to the following hydrometallurgical step. SiO<sub>2</sub> which is used by other authors is purposefully not included as a flux, because it would further complicate the phase system and is less desired than CaO and Al<sub>2</sub>O<sub>3</sub> due to the detrimental formation of silica gel, which increases process complexity and could lead to REE losses [19] in the planned hydrometallurgical step. CaO and Al<sub>2</sub>O<sub>3</sub> consume acid during slag leaching but they are desired to be recovered as fluxes after precipitation.

To estimate the potential content of REE oxides in such a slag system, modelling with the calculation of phase diagrams (CALPHAD) approach [20] lead to phase diagrams with regard to the CaO-Al<sub>2</sub>O<sub>3</sub>-REE<sub>2</sub>O<sub>3</sub> slag. Further information on the respective CALPHAD modelling of this system and on accompanying experimentation is presented in Ilatovskaia et al. (2023) [21]. FeO<sub>x</sub> is not included for phase modelling because if a proper Fe-Nd separation is achieved in the process, Fe should never form oxides or enter the slag phase. Information on the CaO-Nd<sub>2</sub>O<sub>3</sub>-Fe<sub>2</sub>O<sub>3</sub>-Al<sub>2</sub>O<sub>3</sub> system, found in Jantzen and Glasser (1979) [22], is discussed.

Based on the initial findings, a process route is proposed (Figure 1). It comprises a two-step process, because this allows for complete REEs oxidation in the first step and then the reduction of FeO<sub>x</sub> and of the oxides of more noble metals than iron in the second step. A one-step process could also be theoretically possible. Nonetheless, without complete pre-oxidation it is harder to control the exact p(O<sub>2</sub>) over long equilibration times (which are then required) where Fe and B remain in the metallic state, while the alumina flux will be reduced by the REE at process temperatures. The produced Al will then be slagged again to Al<sub>2</sub>O<sub>3</sub>.

Small waste REPMs with a comparably high surface area (thus amount of coating) were used (Figure 2a). The magnets were demagnetized in a muffle furnace at 400 °C with the coating staying mostly intact and subsequently crushed and milled in a closed vibratory disc mill (Figure 2b). The resulting partially oxidized powder has been analyzed via ICP-OES (Varian 725-ES) and CS (Eltra CS 580). Subsequently, this powder is mixed with Al<sub>2</sub>O<sub>3</sub> and CaO at their eutectic composition (0.354 mol Al<sub>2</sub>O<sub>3</sub> to 0.646 mol CaO) following the setups in Table 1. Because the oxidation of REE is highly exothermic, ratios of 1:5 and 1:2.5 (magnets:flux) were chosen for good controllability. Oxidizing pure REPM materials with O<sub>2</sub> in a closed system adiabatically would lead to a temperature of 2100 °C according to HSC Chemistry software calculations.

The experiments have been carried out in a corundum crucible under an ambient atmosphere and pressure in an induction furnace (EMA-TEC, 20 kW). While corundum slowly solutes Al<sub>2</sub>O<sub>3</sub> into the slag, this effect is marginal. A corundum crucible does not introduce new elements to the system and is suitable for the oxidation step (in contrast to graphite or SiC). Heating was slow until the REE started oxidizing with flux bound O<sub>2</sub>; the slag was further heated up to 1500 °C, a corundum lance was subsequently submerged and pressurized dry air was used at 300 L/h for 5 h to fully oxidize all the material at high p(O<sub>2</sub>) into one fully molten slag (Figure 2c). Between setups 1 and 3, the REPM to flux ratio is varied to research the effect of different fluxing amounts. Setup 2 was planned with the addition of P<sub>2</sub>O<sub>5</sub>, in the effort to concentrate REEs in Monazite-like REEs (PO<sub>4</sub>).

**Table 1.** Mixtures for oxidative smelting.

Setup	REPM to Flux Ratio
1	1:5 (200 g REPM powder, 499.1 g Al <sub>2</sub> O <sub>3</sub> and 500.9 g CaO)
2	1:5 & P <sub>2</sub> O <sub>5</sub> (200 g REPM powder, 499.1 g Al <sub>2</sub> O <sub>3</sub> , 500.9 g CaO and 29.8 g P <sub>2</sub> O <sub>5</sub> )
3	1:2.5 (300 g REPM powder, 374.3 g Al <sub>2</sub> O <sub>3</sub> and 375.67 g CaO)

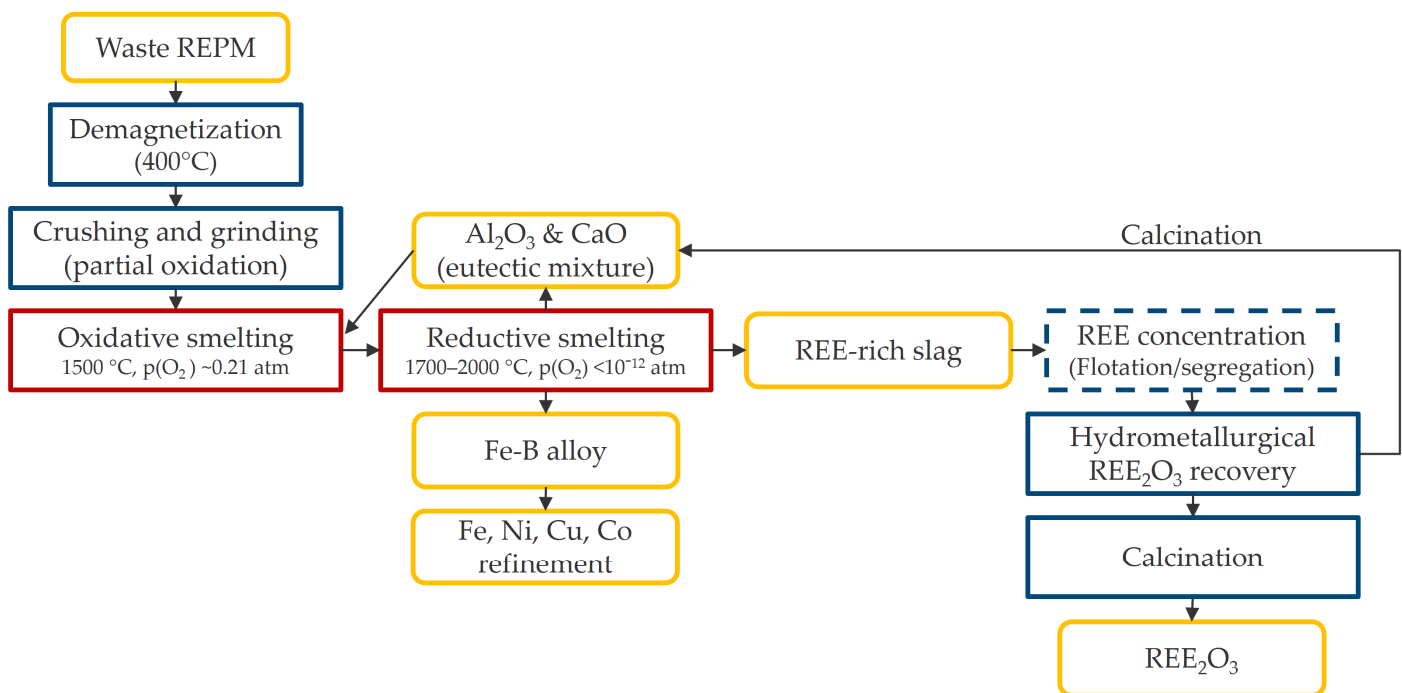


**Figure 1.** Flowchart of the proposed two-step process. Raw REPM waste is demagnetized, grinded and milled, then the prepared magnets are fully mixed with the fluxes (Al<sub>2</sub>O<sub>3</sub> and CaO) and oxidized to form a single slag phase. In the subsequent reductive step, Fe as well as some more noble metals (B and metals from REPM coating) are separated into an Fe phase. The resulting REE oxide-rich phase could be either concentrated further via flotation or segregation or used directly in a hydrometallurgical purification step to produce REE<sub>2</sub>O<sub>3</sub>. These oxides can be further refined to REE metal via molten salt electrolysis. The Al<sub>2</sub>O<sub>3</sub> and CaO could be recovered after decomposition/calcination of respective precipitates and back-cycled as new flux. Since the REE distribution is defined by the REPM, there might be no need to separate Nd, Pr and Dy, because the distribution is already suitable for REPM, while small adjustments can be carried out by adding further REE<sub>2</sub>O<sub>3</sub>.

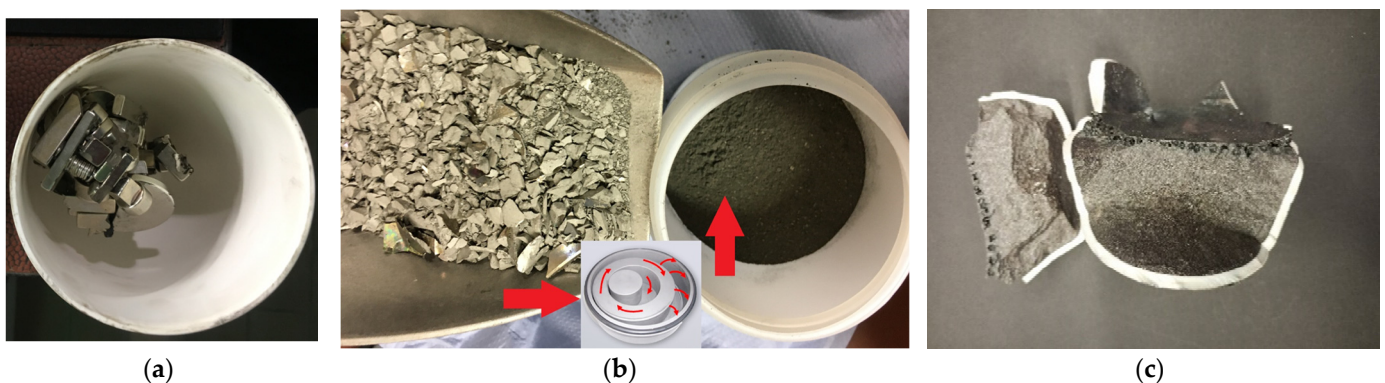


**Figure 2.** (a) The REPM before demagnetization, ((b), left) after crushing and ((b), right) milling as well as (c) the completely oxidized product slag from setup 1.

Next, the resulting fully oxidized mixtures from setups 1 to 3 were analyzed via SEM (Zeiss Ultra 55) with EDX (EDAX), ground down again, analyzed via ICP-OES and then used for reduction experiments (Table 2). These involve a variation of the slag composition to be reduced; temperature, time and reduction agent. Reduction experiments were performed in graphite crucibles within a high-temperature chamber furnace (Carbolite Gero HTK 25GR/25) at 1 atm with Ar flushing. The amount of reduction agent was calculated via FactSage 8.1 [23] for carbothermic experiments and the modelled amount

(4.2 g C for setups 1 and 2; 5.7 g C for setup 3) has been supplied as graphite powder and mixed with the fine-milled slag (100 g). The graphite crucible should allow for larger carbon availability in comparison with the model.

**Table 2.** Mixtures for reductive smelting, utilizing carbothermic and metallothermic methods.

Reduction Setup (RS)	Type	Mixture	T (°C)	Time at T (min)
1	carbothermic	100 g setup 1 slag, CaO, 4.2 g graphite powder.	1800	5
2	Carbothermic	100 g setup 1 slag, CaO, 4.2 g graphite powder.	1800	60
3	Carbothermic	100 g setup 1 slag, CaO, 4.2 g graphite powder.	1900	60
4	carbothermic	100 g setup 1 slag, CaO, 4.2 g graphite powder.	2000	60
5	carbothermic	100 g setup 2 slag, CaO, 4.2 g graphite powder.	1900	60
6	carbothermic	100 g setup 3 slag, CaO, 5.7 g graphite powder.	1900	60
7	metallothermic	100 g setup 1 slag, CaO, 112 g partially oxidized REPM powder	1700	60
8	metallothermic	100 g setup 1 slag, CaO, 112 g REPM magnets (demagnetized)	1700	60

Initial tests were also performed on the metallothermic reduction of the slag with fresh REPM material, using a stoichiometric calculation for oxygen transfer from the  $\text{FeO}_x$  of the slag to the REEs of the fresh magnets. This should (i) lead to a higher overall amount of REEs in the slag, (ii) does not require any carbon-based reduction agent and is  $\text{CO}_2$  neutral and (iii) more REPM is directly recycled without the requirement for a fine-tuned  $p(\text{O}_2)$  calibration and long holding times. To account for partial oxidation while crushing and grinding, 50% excess REPM powder was used, leading to 112 g REPM powder per 100 g of setup 1 slag. To compare the above experiment while using magnets directly without a pre-treatment, the same procedure was realized using whole demagnetized cylindrical (height 5 mm, diameter 3.5 mm) REPM magnets. Subsequent to reductive smelting, the crucibles were broken, the metal phase was separated from the slag phase and both were analyzed via CS, ICP-OES and SEM-EDX.

To prove the feasibility of the generated slags in terms of recovering  $\text{REE}_2\text{O}_3$ , CaO and  $\text{Al}_2\text{O}_3$ , selectively initial tests on artificial pure oxide mixtures were carried out to study the respective hydrometallurgical processing. Two proposed routes were examined within this work on the basis of leaching and precipitation with the use of sulfuric acid while recovering REE double sulfates and methane sulfonic acid while recovering REE hydroxides. Therefore, synthetic slags exhibiting a composition of 44 wt. % CaO, 46 wt. %  $\text{Al}_2\text{O}_3$  and 10 wt. %  $\text{Nd}_2\text{O}_3$  were produced to simulate a potential slag after the reductive pyrometallurgical step. The aim of this study was to define the optimal parameters for the selective precipitation of REEs; salts and fluxes after slag leaching.

In the first series of experiments, 1000 mL of 20 g/L single element solutions of Nd, Ca or Al were prepared by dissolving either oxide (for Nd and Ca) or metal (for Al) in an acidic solution with 1 M final acidity. The purities of the feed materials were  $\text{Nd}_2\text{O}_3 > 99$  wt. %, CaO  $> 97$  wt. % and Al  $> 99.9$  wt. %. The investigated solvents were hydrochloric acid, nitric acid, sulfuric acid and methane sulfonic acid (MSA). In the next step, the precipitation of Nd, Ca and Al from the respective solutions was studied. A 100 mL solution was stirred at 300 rpm in a beaker and 5 M NaOH or 25% ammonia solution was added. The pH was continuously measured, and 1 mL samples were taken periodically to determine the elemental concentration over time and define the optimum pH values for selective precipitation.

In a second series of experiments, the above-mentioned synthetic slag mixture of 44 wt. % CaO, 46 wt. % Al<sub>2</sub>O<sub>3</sub> and 10 wt. % Nd<sub>2</sub>O<sub>3</sub> was produced. Slag components were dried at 120 °C for 24 h, weighed, mixed and smelted at 1650 °C for 30 min under an argon atmosphere using an induction furnace. The solidified slag was mechanically separated from the crucible, milled in a vibration disc mill and sieved to <200 µm particle size. Leaching was performed in borosilicate flasks with silicon stoppers to prevent evaporation. Respective amounts of slag were leached for 120 min in 100 mL of sulfuric or methane sulfonic acid while being stirred at 300 rpm. Samples were taken after 5, 10, 15, 20, 30, 60, 90 and 120 min. Solid:liquid (s:l) ratios of 20, 40, 60, 80 and 100 g/L, temperatures of 25, 40, 60 and 80 °C and acid concentrations of 2, 4 and 6 M were studied to determine the optimum leaching parameters. Subsequently, 450 g slag were leached in both acids under prior defined optimum conditions. Solid/liquid separation was conducted by a centrifuge. An amount of 5 M NaOH or 25% ammonia solution was added to the solution to selectively precipitate the Nd, Ca and Al at the respective pH values defined in the first series of experiments.

### 3. Results

#### 3.1. Modelling Results

The thermodynamic database of the CaO-Al<sub>2</sub>O<sub>3</sub>-Nd<sub>2</sub>O<sub>3</sub> system was developed by Ilatovskaia et al. (2023) [21] using thermodynamic descriptions of binary systems and adjusting the thermodynamic functions of  $\tau_2$  (NdCaAl<sub>3</sub>O<sub>7</sub>) and  $\tau_2$  phases to reproduce the phase diagram presented in the work of Janzen and Neugaonkar (1981) [24] at 1300 °C. It should be kept in mind that this database is preliminary and needs further optimization based on experimental data, e.g., the melting temperature of the  $\tau_2$  phase studied experimentally in [21] was obtained to be higher than in calculations. The calculations were performed using Thermo-calc software [25]. According to the calculations and resulting phase diagrams shown in Figure 3, the homogeneity range of the liquid phase can extend above 20 wt. % at 1700 °C. Therefore, slag containing 20 wt. % will be completely molten forming  $\tau_1$ ,  $\tau_2$  and NdAlO<sub>3</sub> in the process of solidification. The formation of these phases can already be observed at 1500 °C. Experimental investigations of samples with compositions in three-phase fields  $\tau_2 + C3A + CA$ ,  $\tau_2 + CA + CA2$  and  $\tau_1 + \tau_2 + C3A$  showed that they were completely melted at 1600 °C [21]. Microstructure investigations of the molten samples indicated a non-equilibrium character of solidification and that the even formation of NdAlO<sub>3</sub> highly concentrating Nd was observed.

Because a certain degree of solids could still be feasible in a molten process, they are relevant. They also define which Nd<sub>2</sub>O<sub>3</sub>-bearing minerals form in the course of slow cooling of the slag. At 1500 °C, a completely liquid slag can optimally only contain around 7 wt. % of Nd<sub>2</sub>O<sub>3</sub> (which is the appropriated representative for all REE oxides). At 1700 °C however, a liquid slag with up to around 25 wt. % of Nd<sub>2</sub>O<sub>3</sub> can be achieved; also the Nd<sub>2</sub>O<sub>3</sub>-rich NdAlO<sub>3</sub> phase (>75 wt. % Nd<sub>2</sub>O<sub>3</sub>) can be precipitated from such a slag. Theoretically, a slag system with some solid NdAlO<sub>3</sub> might still be workable even at Nd<sub>2</sub>O<sub>3</sub> contents above 25 wt. %.

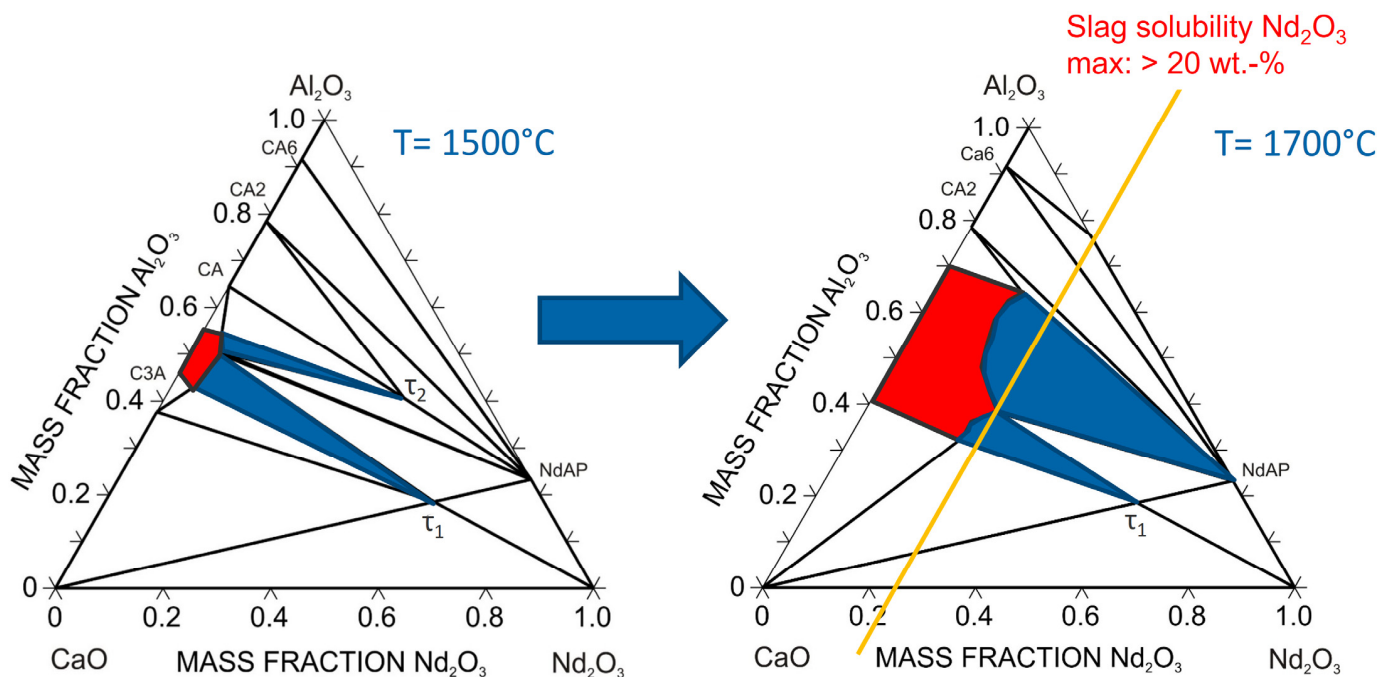


**Figure 3.** Phase diagrams of the CaO-Al<sub>2</sub>O<sub>3</sub>-REE<sub>2</sub>O<sub>3</sub> system at 1500 °C (left) and 1700 °C (right). The stability field of the liquid single phase is marked red, while two-phase regions, which include a liquid slag and a Nd<sub>2</sub>O<sub>3</sub>-rich mineral ( $\tau_1$ : NdCaAlO<sub>4</sub>;  $\tau_2$ : NdCaAl<sub>3</sub>O<sub>7</sub>; NdAP: NdAlO<sub>3</sub>) phase, are blue.

### 3.2. Pyrometallurgical Process

The magnets show a typical [5] composition for small REPM magnets (Table 3). Crushing and milling leads to a fine powder. When opening the vibratory mill fast after use, while the powder is still hot, a clear burn-off is observed. Hence, to avoid full oxidation, the powder is given time to cool first before opening the mill. The composition of the slags after smelting, including the respective fluxing of the magnets, are shown in Table 3 for the setups investigated.

**Table 3.** ICP-OES for the feed REPM (elements in metallic form) and the oxidized slags (setup 1–3; cf. Table 1, all elements in oxidic form).

Element	Feed REPM (wt. %)	Setup 1 (wt. %) (1 <sub>[REPM]</sub> :5 <sub>[flux]</sub> )	Setup 2 (wt. %) (1 <sub>[REPM]</sub> :5 <sub>[flux]</sub> + P <sub>2</sub> O <sub>5</sub> )	Setup 3 (wt. %) (1 <sub>[REPM]</sub> :2.5 <sub>[flux]</sub> )
Al	0.54	24.89	22.54	20.86
B	0.74	0.13	0.13	0.19
Ca	-	20.81	23.74	20.40
Cu	0.26	0.02	<0.01	0.03
Dy	0.08	0.01	0.01	0.01
Fe	68.94	10.93	9.51	14.66
Nb	0.17	0.03	0.02	0.04
Nd	21.81	3.16	2.92	4.52
Ni	0.26	0.10	0.01	0.09
P	-	-	0.87	-
Pr	7.15	1.04	0.93	1.47

The SEM-EDX results obtained are in accordance with those obtained by the ICP-OES analysis, showing a concentration of around 4 wt. % REEs for setup 1 and 2 and around 6 wt. % for setup 3, when analyzing large areas of slag samples. The main mineral phases (Figure 4) for setups 1–3 are a (Nd,Pr)CaAl<sub>3</sub>O<sub>7</sub> phase ( $\tau_2$ ), a CaAl<sub>2</sub>O<sub>4</sub> (CA2) phase and

an Fe-rich oxide phase. The REEs mainly concentrate in the  $\tau_2$  phase ((Nd,Pr)CaAl<sub>3</sub>O<sub>7</sub>; Figure 5) which contains more than 40 wt. % of REE. The oxidized slags seem relatively homogeneous. However, due to cooling effects, the mineral phases are much bigger and more defined towards the center of the crucible, with the CaAl<sub>2</sub>O<sub>4</sub> phase (forming spike-like monoclinic structures),  $\tau_2$  phase (forming tetragonal structures) and the orthorhombic Brownmillerite Ca<sub>2</sub>(Al,Fe)<sub>2</sub>O<sub>5</sub> phase being mainly present.

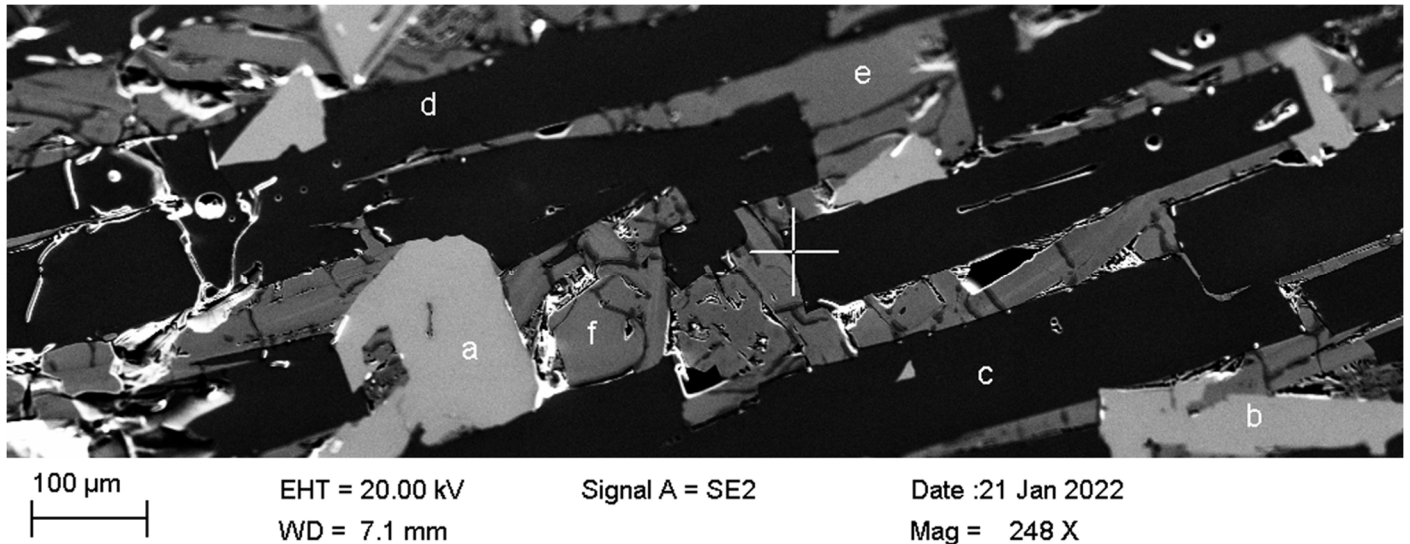


**Figure 4.** SEM image magnified 250 times of the resulting slag of setup 3 (magnet to slag ratio of 1:2.5), showing the three main phases in the Fe-rich fully oxidized slags. REEs concentrate mainly at (a,b), i.e., within  $\tau_2$  (cf. Figure 3; (Nd,Pr)CaAl<sub>3</sub>O<sub>7</sub>). Phases (c,d) represent a CaAl<sub>2</sub>O<sub>4</sub> (CA2) phase which always contains below 2 wt. % of REEs, while (e) represents a chemically more variable Fe oxide-rich phase (brownmillerite) that can concentrate REEs up to 9 wt. %. Some Fe oxides (magnetite) with small amounts of Al, Ca and Co are also present (f).

The addition of P<sub>2</sub>O<sub>5</sub> within setup 2 has no noteworthy effect; P reports to the Fe-Ca-Al phase up to 3 wt. %, around 12 wt. % into a rare Ca-P-O phase and only 0.1 wt. % into  $\tau_2$ . The concentration of REEs in silico-phosphate phases as in [10] requires the presence of SiO<sub>2</sub>, while monazite formation was not observed.

The results of the reduction experiments lead to a phase separation of an Fe-rich metal phase and an oxidic REEs collector slag phase. The chemical composition of these phases is shown in Table 4 below. For some setups, images (Figure 6) are shown. At temperatures of 1800 °C–2000 °C, Al<sub>2</sub>O<sub>3</sub> can be reduced in a carbothermic manner within the slag, leading to Al entering the metal phase. The respective Al metal phase concentration (taken from SEM-EDX values) is shown in Figure 7 for the RS1-4 slags in dependence of the parameters' temperature and time. SEM images for the reduction in setup 1 and 6 are shown in Figure 8.



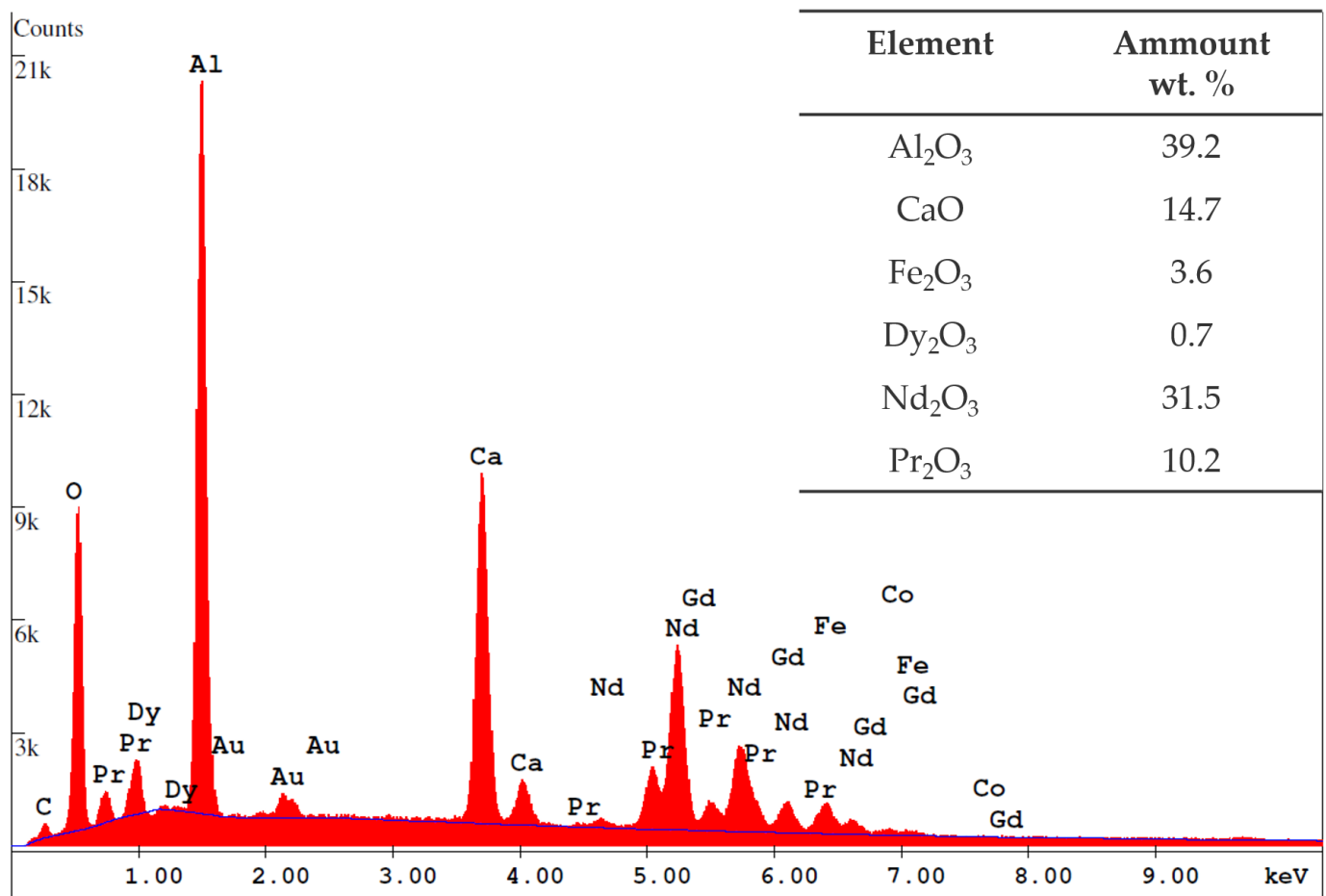


**Figure 5.** The  $\tau_2$  phase ((a) in Figure 4) contains around 30 wt. % Nd, 10 wt. % Pr and 0.7 wt. % Dy (>40 wt. % REE), 24 wt. % Al, 12 wt. % Ca, 3 wt. % Fe, some Co and oxygen. C and Au are artifacts from handling and coating. B is not traceable with the utilized EDX. Oxygen values are calculated, due to high uncertainty in EDX determination.

**Table 4.** ICP-OES and CS results for the slag (oxidic) and SEM-EDX results for the metal phases of each of the six carbothermic reduction experiments. SEM-EDX results are not representative for the complete phase, especially for low concentrations and cannot analyze boron.

Element	RS 1 Slag	RS 1 Metal	RS 2 Slag	RS 2 Metal	RS 3 Slag	RS 3 Metal	RS 4 Slag	RS 4 Metal	RS 5 Slag	RS 5 Metal	RS 6 Slag	RS 6 Metal
Al	25.92	3.13	24.51	5.22	26.45	10.10	24.79	23.96	23.96	13.78	24.53	12.28
B	0.05	-	<0.01	-	0.01	-	<0.01	-	0.08	-	0.01	-
Ca	26.885	-	4.83	-	27.57	-	27.25	-	22.62	-	25.13	-
Cu	<0.01	-	<0.01	-	<0.01	-	<0.01	-	0.07	-	<0.01	-
Dy	0.01	-	0.01	-	0.01	-	0.01	1.30	0.01	-	0.02	-
Fe	2.56	92.50	2.06	91.00	0.45	86.22	1.54	69.90	11.94	82.68	0.35	84.28
Nb	0.01	0.16	0.01	-	0.01	-	0.01	0.24	<0.01	-	<0.01	-
Nd	3.16	0.09	2.93	-	3.34	0.10	3.27	0.05	2.67	0.17	5.81	0.08
Ni	0.01	0.25	0.01	0.33	<0.01	-	<0.01	-	0.04	-	<0.01	0.36
P	-	-	-	-	-	-	-	-	0.76	<0.01	-	-
Pr	1.00	-	0.97	-	1.06	0.07	1.05	-	0.90	0.11	1.95	0.11

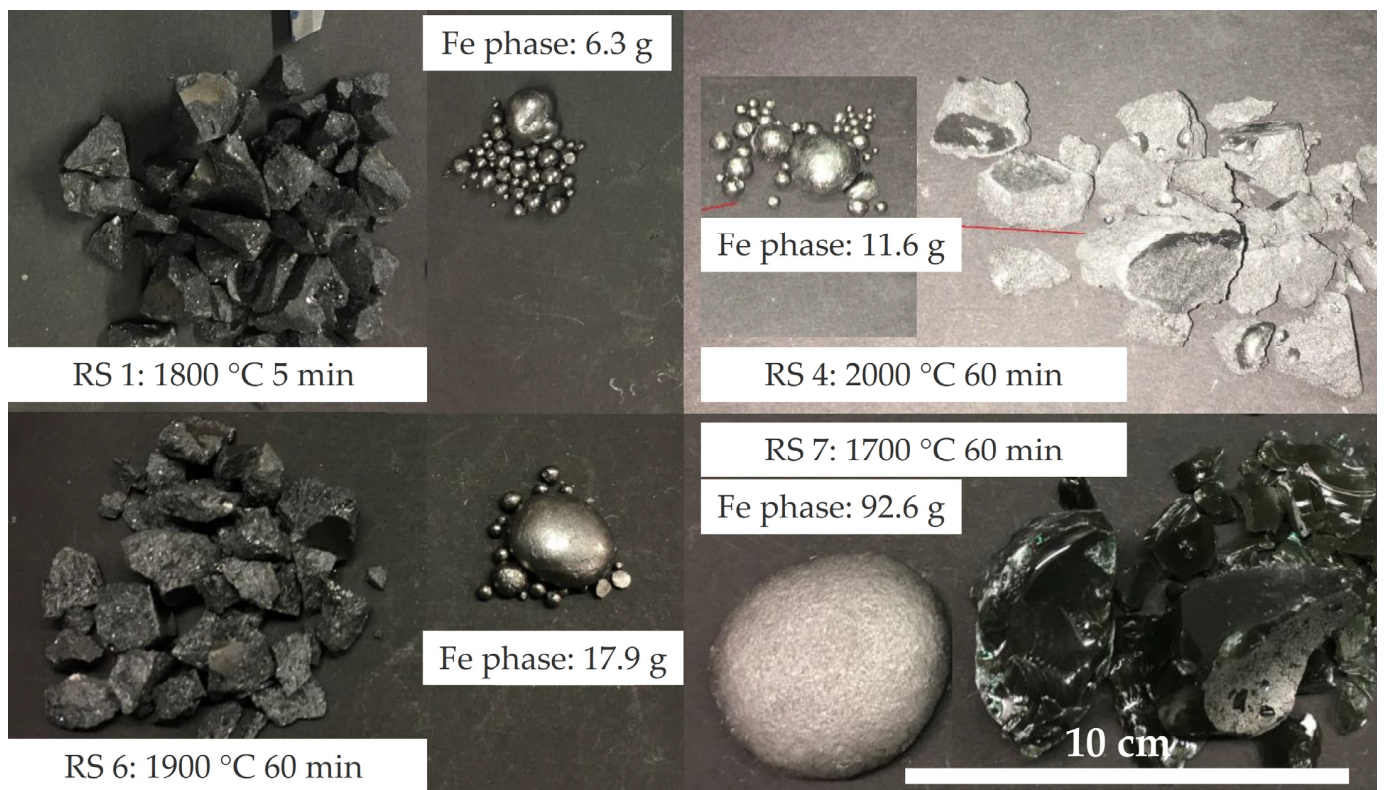


Figure 6. Images of the product phases from the reduction setups 1, 4, 6 and 7.

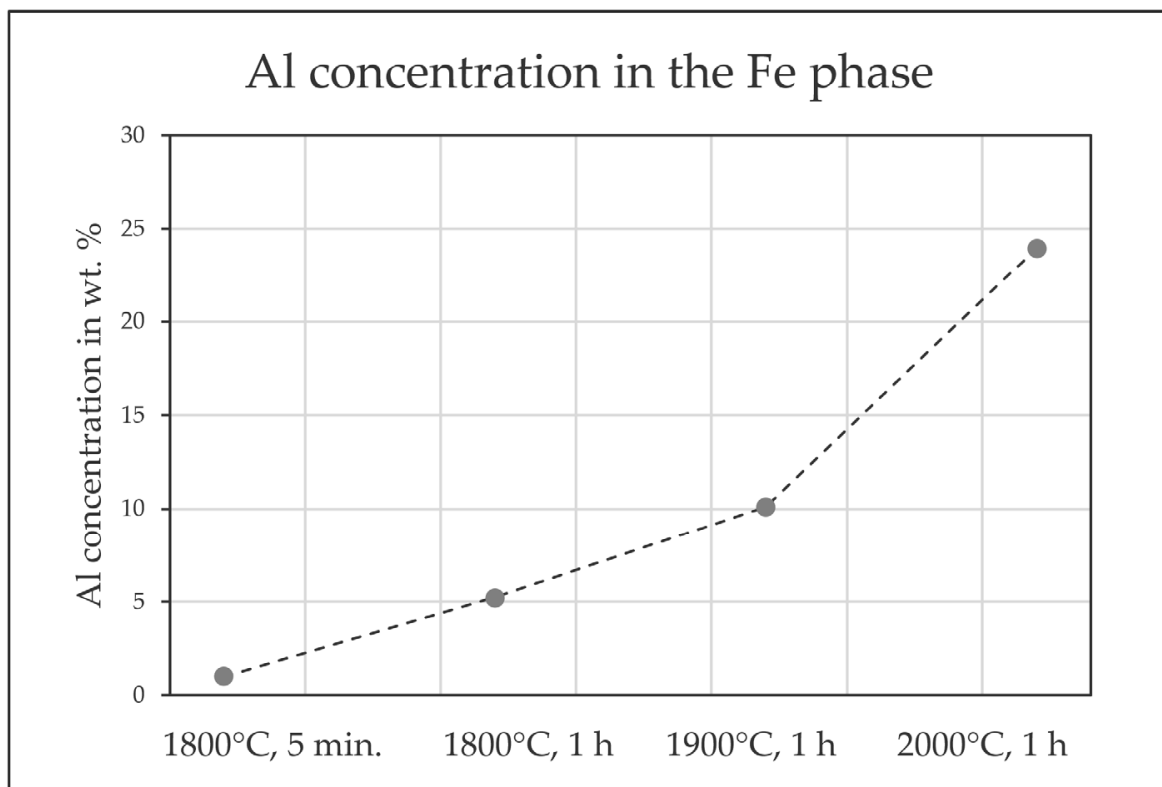
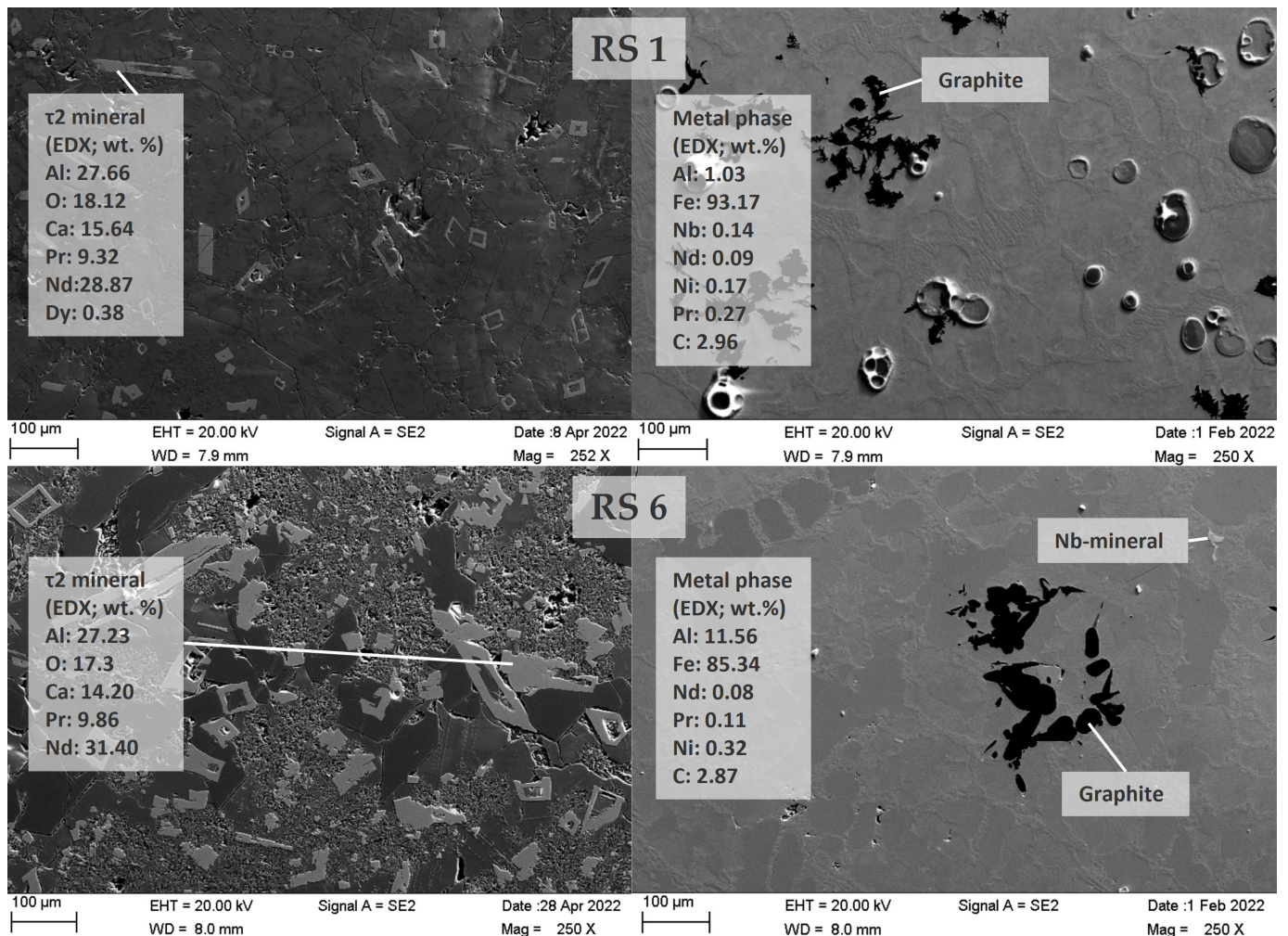


Figure 7. Al concentration in the Fe phases after carbothermic reduction with different conditions.



**Figure 8.** SEM images magnified 250 times of the reduction product from RS 1 (upper) and RS 6 (lower) are shown.

While only 54% of the contained Fe (setup 1 contains 10.9 g Fe in 100 g, cf. Table 3) is separable in RS 1, with a longer holding time (60 min) and higher temperature (2000 °C) in RS 4 Fe separation already increases to 82%. For RS 6, at 1900 °C the Fe yield was even higher, probably due to a better collectability of Fe when more is available within the crucible. The Fe phases are not pure and contain C and Al. Finally, for the metallothermic reduction the separability of the Fe phase was by far the best, reaching values of 95%. The slags of RS 7 contain 18.5 wt. % REEs, which is equal to around 21.6 wt. % REE oxides. RS 8 performed similarly. Since a major Si contamination is observable in RS 7 and 8, this is not yet proof for a REEs load above 20 wt. % in pure Al-Ca-Nd-O slags, but points toward it.

The RS 1 and 6 slags show the same  $\tau_2$  mineral as the oxidized slags. No NdAP is found. While the Ca-Al oxides are still rather REE-lean, they can now concentrate up to around 5 wt. % of REEs. Fe is mostly non-detectable in both samples. The RS 6 slag shows more  $\tau_2$ ; in accordance with the lower flux amount, more fine crystalline phases without clear mineral formation are common. In general, the amount of Fe is low in the slags. Both metal phases are carbon-saturated, and graphite segregates while cooling. The RS 6 metal phase contains around 11.5 wt. % Al, which is in accordance with RS 3 (both 1900 °C, 60 min) and caused by a reduction of  $\text{Al}_2\text{O}_3$  from the flux. Nb was found to form small Nb-rich minerals in the metal phase.

### 3.3. Hydrometallurgical Process

The first series of hydrometallurgical experiments were realized to determine the practical pH values for the elemental precipitation of Nd, Ca or Al salts from hydrochloric, nitric, sulfuric and methane sulfonic acid solutions due to an addition of 5 M NaOH or 25%  $\text{NH}_4\text{OH}$ . Since  $\text{CaSO}_4$  is hardly soluble, the precipitation of Ca was only tested in HCl,  $\text{HNO}_3$  and MSA. Below pH 12, no significant precipitation was visible. As demonstrated in Figure 9,  $\text{Al}(\text{OH})_3$  precipitates in HCl,  $\text{HNO}_3$  and MSA between pH 3 and 6. In sulfuric acid, Al precipitation starts at pH 1 which is concluded through the formation of double sulfates of  $\text{Al}_2(\text{SO}_4)_3$  with  $\text{Na}_2\text{SO}_4$  or  $(\text{NH}_4)_2\text{SO}_4$ , respectively, while ammonia salts precipitate faster at a lower pH. Precipitation completes at pH 5 after hydroxide formation. As demonstrated in Figure 10, Nd also behaves differently in  $\text{H}_2\text{SO}_4$ . The addition of 5 M NaOH leads to >95% precipitation at pH 2. This is also concluded by the formation of hardly soluble neodymium sodium double sulfates ( $\text{NaRE}(\text{SO}_4)_2 \cdot \text{H}_2\text{O}$ ). The addition of an ammonia solution does not lead to significant precipitation of double sulfates despite contradicting accounts from the literature [26]. Low Nd concentrations in an inadequate nucleation time may be the reason. For the other acids and for ammonia in sulfuric acid,  $\text{Nd}(\text{OH})_3$  starts precipitating around pH 6 and completes at pH 8.

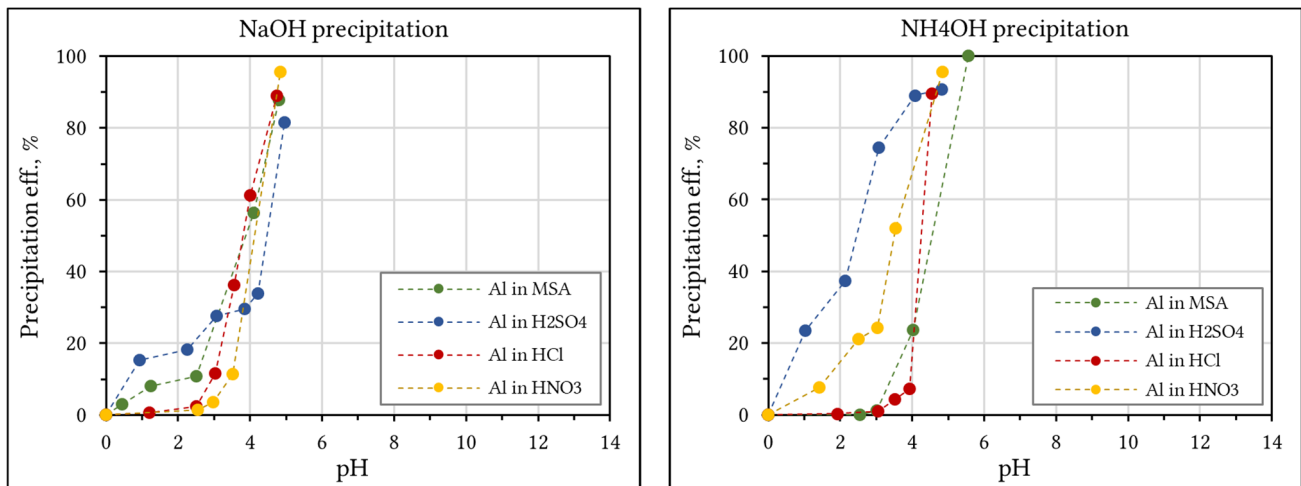


**Figure 9.** Precipitation of Al from  $\text{H}_2\text{SO}_4$ , MSA, HCl and  $\text{HNO}_3$  at different pH values due to addition of NaOH or  $\text{NH}_4\text{OH}$ .

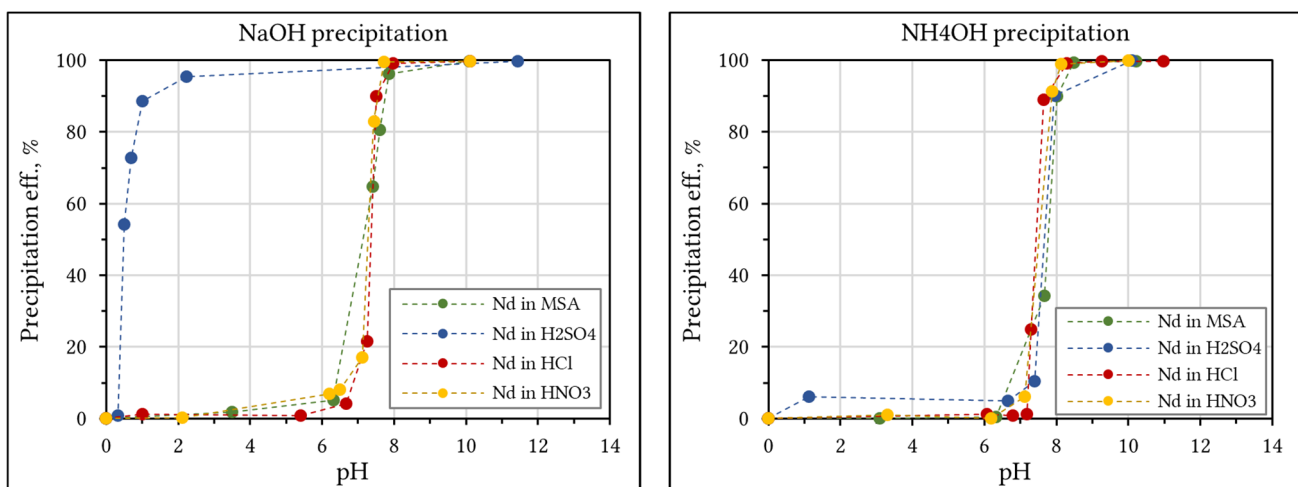


**Figure 10.** Precipitation of Nd from  $\text{H}_2\text{SO}_4$ , MSA, HCl and  $\text{HNO}_3$  at different pH values due to addition of NaOH or  $\text{NH}_4\text{OH}$ .

Based on the precipitation behavior of the single salts, the selectivity of multiple precipitation steps was studied in a mixed elemental solution. Therefore, a synthetic slag mixture of 44 wt. % CaO, 46 wt. % Al<sub>2</sub>O<sub>3</sub> and 10 wt. % Nd<sub>2</sub>O<sub>3</sub> and <200 µm particle size was leached under before-determined optimum leaching conditions of 40 °C, 4 M acid and a 60 g/L bulk concentration. Since precipitation in HCl, HNO<sub>3</sub> and MSA showed similar results, only MSA was compared to H<sub>2</sub>SO<sub>4</sub> since it is biodegradable, more environmentally friendly and less corrosive than HCl and HNO<sub>3</sub> [27].

### 3.3.1. Leaching and Precipitation of Synthetic Slag in H<sub>2</sub>SO<sub>4</sub>

Leaching of the slag in 4 M H<sub>2</sub>SO<sub>4</sub> at 40 °C and 60 g/L resulted in the complete dissolution of Al, while 97% of the Ca precipitates as solid gypsum. The process steps are visible in Figure 11. About 24% of the Nd co-precipitated in the gypsum phase, which indicates a double salt formation of neodymium with calcium sulfate since aluminum sulfate does not interfere with the gypsum phase. However, a phase characterization was not performed to validate the statement. After solid–liquid separation, 5 M NaOH was added until pH 1.5 where 98% of the Nd precipitated as sodium double sulfate. The ICP-OES analysis showed impurities of 7.7 wt. % Na, 2.5 wt. % Ca and 0.5 wt. % Al. An increase to pH 7.5 resulted in the complete precipitation of Al(OH)<sub>3</sub> containing 1 wt. % Ca and 0.5 wt.% Nd. The addition of ammonia did not result in the double sulfate formation of Nd and was unsuitable for selective separation.

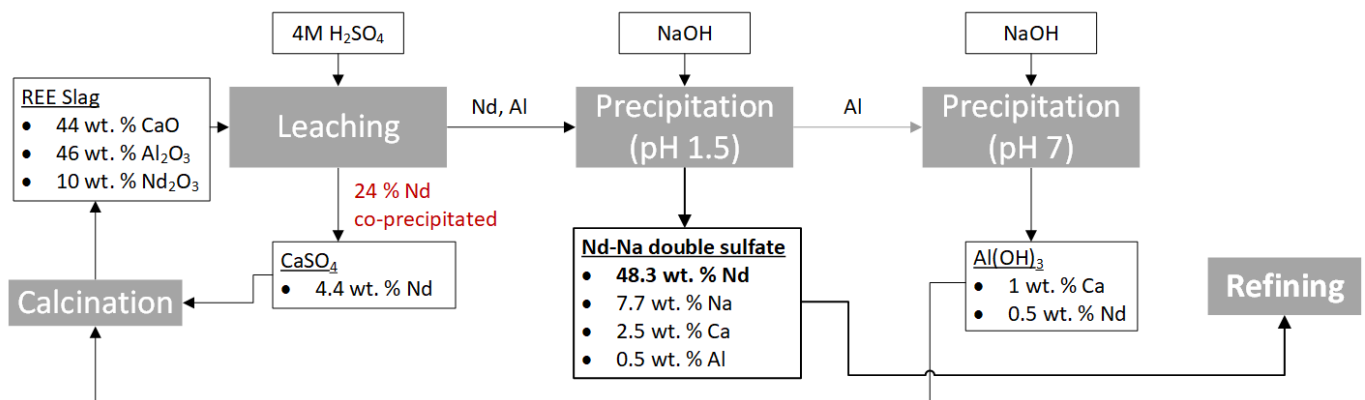


**Figure 11.** Nd and flux recovery from REE slags via sulfuric acid route.

### 3.3.2. Leaching and Precipitation in MSA

Leaching of 60 g/L slag in 4 M MSA at 40 °C resulted in the complete dissolution of Al, Ca and Nd while fine graphite particles from the crucible remained undissolved. An amount of 5 M NaOH or 25% NH<sub>4</sub>OH was added aiming to selectively precipitate Al(OH)<sub>3</sub> at pH 5 and Nd(OH)<sub>3</sub> at pH 8. However, pH control in the neutral region was difficult due to the spontaneous nucleation of hydroxides. As a result, the first precipitation step for NaOH and NH<sub>4</sub>OH was at pH 6. Al fully precipitated along with >95% and >93% Nd for NaOH and NH<sub>4</sub>OH, respectively. The results indicate the fast non-selective co-precipitation of Nd(OH)<sub>3</sub> in the presence of Al(OH)<sub>3</sub>; thus, further refining of the hydroxide mixture is needed. Ca salts such as carbonates or oxalates can be recovered for reuse as flux as the final step. The proposed route is shown in Figure 12.

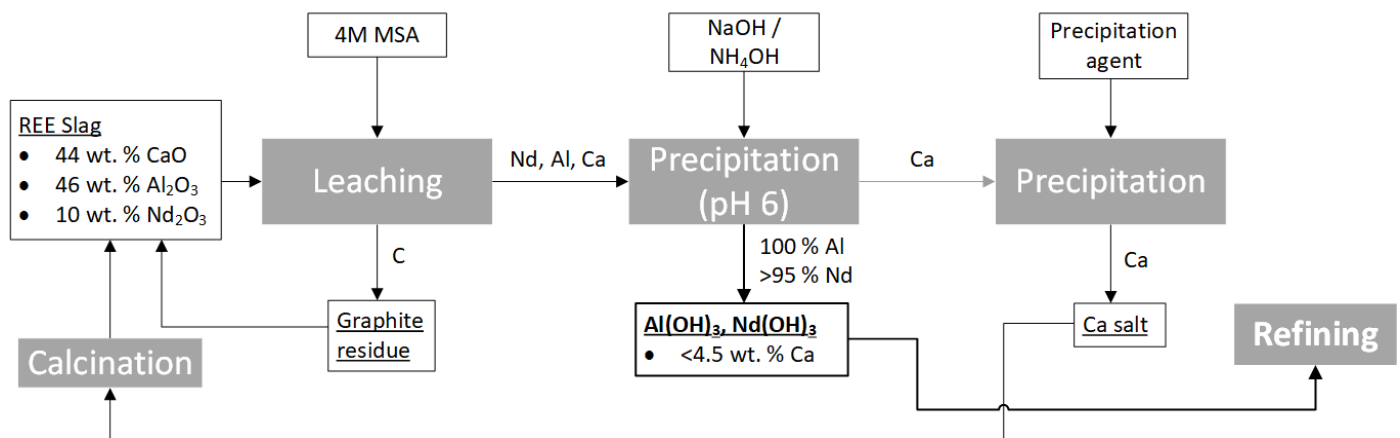


Figure 12. Nd recovery from REE slags via methane sulfonic acid route.

#### 4. Discussion

The calculated phase diagram indicates an overall  $\text{REE}_2\text{O}_3$  saturation of liquid above 20 wt. % at 1700 °C. This is relatively low compared to the initial load of around 29 wt. % (cf. Table 3, feed REPM); however, at temperatures above 1700 °C and while accepting certain amounts of solid REE-rich minerals in the melt, higher REE concentrations can be reached.

The grinding and milling (in a closed mill) are easily realized, but partial oxidation was not avoidable. While this reduces the heating contribution during the oxidized slag formation step, it makes the reaction much more controllable. The reductive experiment 8 with unoxidized, still-coated magnets exhibited a much more turbulent reaction. In a larger scale process, there is no need for grinding; hence, the full energy potential of the process could be utilized.

During oxidative smelting, three fully molten slags containing around 4 wt. % REEs in the setup 1 and 2 slags and 6 wt. % of REEs for the setup 3 slag were achieved at 1500 °C. The load of ~29 wt. % REEs in the REPM is thus reduced during oxidation, but an increase in concentration to above 35 wt. % in  $\tau_2$  (42.4 wt. %  $\text{REE}_2\text{O}_3$ , cf. Figure 5) is already achieved. Utilizing flotation, segregation or melt filtration [28] to concentrate the REEs at this point would prove inefficient, because large quantities of REEs are bound to the Fe-rich phase.

The reduction yielded promising results in all cases, with an Fe lean slag and an Fe rich metal phase being formed. In general, the workability of the carbothermic process is better at a higher temperature. This is mainly due to the better separability of the Fe phase and not the degree of Fe reduction, which is high in all cases. The setup 3 slag at 1900 °C and at an experiment duration of 60 min showed the best results and Fe separation is clear. This is probably due to the overall higher Fe concentration in setup 3 owing to the higher magnet to flux ratio, equal to 1:2.5, of this setup. Consequently, the REE concentration in the slag is the highest in setup 3 compared to the other carbothermic setups. Thus, an even lower fluxing amount than in setup 3 seems promising, especially when working above 1700 °C. This is important, since for the carbothermic setups, even the setup 3 slag contained only 8 wt. % REE (~9.3 wt. %  $\text{REE}_2\text{O}_3$ ) after Fe removal. The oxidative step might then be realized at slightly higher temperatures.

At all temperatures, nearly no Nd (max. 0.17 wt. %) was found in the Fe phase and only little Fe (max. 2.6 wt. %) in the slag phase. Next to the overall higher energy demand and harsher conditions for furnace refractory when working at higher temperatures, in this system  $\text{Al}_2\text{O}_3$  can be reduced in a carbothermic manner. Reduction setup 6 (1:2.5 ratio, 1900 °C and 60 min) has the overall highest amount of REEs in the resulting slag, while only containing 0.1 wt. % Nd in the metal phase and 0.4 wt. % Fe in the slag phase. This makes it the overall most successful attempt at carbothermic reduction. The amount of Al in the Fe phase increases with longer holding times and higher temperatures (up to

24 wt. % at 2000 °C). This could be avoided by using less reduction agent mass and an inert crucible or an overall larger amount of mass compared with a crucible surface. Some Al in the Fe phase (cf. Figure 7) could also be separated by re-smelting with O<sub>2</sub> input, since Al is less noble than Fe. Other value metals (Cu, Ni and Nb) are also concentrated in the Fe phase. B mainly reports to the Fe phase as expected [29]. A process optimization that leads to either transfer into the slag or complete fuming for later separation could be attempted. In general, the process seems more promising at temperatures below 1800 °C, because in the reduction setup 1 most Fe was already reduced from the slag and little Nd remained in the metal phase. The issue of phase separability can most likely be avoided when working on larger scales. No NdAlO<sub>3</sub> was found in the slag; this means that  $\tau_2$  remains the REE richest mineral with around 40 wt. % of REEs, which if separated via flotation, segregation or melt filtration would lead to an increase of the original REE grade from 29 wt. % in the REPM to around 40 wt. % while also facilitating simpler hydrometallurgical downstream processing. When aiming for NdAlO<sub>3</sub> within the slag, slow cooling with the applied REE load would always lead to phase transformation generating  $\tau_2$ , because there is not enough REE to form NdAlO<sub>3</sub>. NdAlO<sub>3</sub> can only be formed if cooling a slag with above 20 wt. % REE<sub>2</sub>O<sub>3</sub> down to around 1700 °C or below from a higher temperature and then quenching the slag.

Discussing the initial findings of the metallothermic reduction setups (RS 7 and 8), it is shown that in both cases the separation of Nd and Fe was successful, while only utilizing more REPM and no carbon-based (and thus CO/CO<sub>2</sub> emitting) reduction agent. This was already achieved at 1700 °C. Because of the strong exothermic reaction, local temperatures might have exceeded 1700 °C. The analysis shows higher amounts of Si in both slag and metal. While this is a contamination that already occurred during the oxidative step, we believe the metallothermic approach is also promising for the CaO-Al<sub>2</sub>O<sub>3</sub>-REE<sub>2</sub>O<sub>3</sub> system. In the featured experiments, SiO<sub>2</sub> behaved like a further flux, leading to crucible overflow, furnace shutoff and fast cooling into a glassy slag phase. Since the metallothermic process requires no carbon-based reduction agent, it is CO<sub>2</sub> neutral, making it the superior choice for possible industrial applications compared with the carbothermic process.

While conditions to form Nd carbides are met [30], they are not found in the SEM images. Further lowering of the process temperatures (below 1700 °C) could be attempted, especially when decreasing the liquidus temperature by adding further fluxes, which do not inhibit the hydrometallurgical step.

The metallothermic process already indicates that a one-step process could be achievable. Here, oxygen could be supplied either as a gas when working under controlled p(O<sub>2</sub>) or chemically bound to oxidize the Nd from REPM into the CaO-Al<sub>2</sub>O<sub>3</sub> slag. If slightly less oxygen is provided, Al would be found in the metal phase. This is preferable in comparison with stronger oxidation, leading to an incomplete Fe-Nd separation and FeO<sub>x</sub> in the slag.

When comparing the featured process to primary REE production, the typical concentration for REE oxides in ores of around 5 wt. % [31] was exceeded at around 9.3 wt. % in the best carbothermic setup (RS 6) and at around 18.5 wt. % for the best metallothermic setup (RS 7). Comparing  $\tau_2$  to REE-bearing minerals such as monazite, the concentration is lower at around 42 wt. % REE<sub>2</sub>O<sub>3</sub> compared to 65–70 wt. %. However, this “artificial ore” would not suffer from the radioactive components often associated with REE ores and the Nd to Pr and Dy ratio is already optimized for REPM; no La or Ce is present.

The leaching of Nd, Ca and Al from synthetic slags and selective separation by the addition of NaOH and NH<sub>4</sub>OH was investigated for simple hydrometallurgical separation of the slag components. Leaching in H<sub>2</sub>SO<sub>4</sub> results in a gypsum phase while 24% Nd co-precipitated. The high loss of Nd can be prevented by calcination of the gypsum phase and reused as flux in slag smelting where Nd is again recovered in the slag. However, this approach has disadvantages such as: energy costs for Nd and gypsum calcination and decreased capacities for fresh magnets in slag smelting. Nonetheless, the calcination step could be realized “in situ”, i.e., by the addition of the precipitates during magnet smelting, thus making use of the heat released during magnet oxidation. The remaining Nd in the

solution can be precipitated as double sulfate by the addition of NaOH. However, 7.7 wt. % Na, 2.5 wt. % Ca and 0.5 wt. % Al in the product require further purification. Neodymium oxalate or carbonate precipitation was not investigated but is a potential alternative. A second refining step is still assumed due to the co-precipitation of the remaining Ca.

In 4 M MSA, all slag components were fully dissolved. The co-precipitation of  $\text{Al}(\text{OH})_3$  and  $\text{Nd}(\text{OH})_3$  at pH 6 was found to precipitate 100% Al and >94% Nd and only 1.5% Ca. Refining of the hydroxide in a second step may be achieved by leaching and selective precipitation of neodymium salts such as oxalates or carbonates. The remaining calcium in the solution can be precipitated, e.g., as carbonate or oxalate and reused as flux after calcination. The reuse of Ca and Al as flux poses a significant advantage of the process compared to the direct leaching of magnets where iron precipitates are typically lost. Moreover, any loss of neodymium to the Ca and Al intermediates will be reprocessed in the pyrometallurgical step as well. Leaching with MSA seems to be beneficial compared to sulfuric acid due to high losses of neodymium to the gypsum phase. However, the refining of hydroxides from the MSA route must be investigated. Alternatively, ion exchange or solvent extraction could be used to separate Ca, Al and Nd. In general, solvent extraction is needed if the separation of Nd from other REEs, such as Dy, is required. In that case, additional separation steps for Ca and Al removal seem feasible.

Further work should consider demonstrating the recovery of mixed REE oxides from actual REPM waste-generated slags. Real slags may accumulate impurities such as a dissolved metal phase or ferrous oxide, which were not investigated in this research. In addition, molten salt electrolysis to produce a REE alloy, potentially of adjusted composition by further REE oxide, is critical for the success of this approach. Finally, melt filtration experiments are considered a potential approach for the recovery of REE-rich mineral phases from the slags present in the pyrometallurgical steps.

## 5. Conclusions

- A two-step pyrometallurgical process separating Fe and Nd from REPM was successfully implemented leading to a homogeneously oxidized slag. After subsequent carbothermic reduction, an iron lean slag concentrating 9.3 wt. % REE oxides was successfully generated at 1900 °C. During metallothermic reduction, with the use of fresh magnets as the reductant stream, a slag of 21.6 wt. % REE oxides was generated at 1700 °C.
- The produced slag phase is Fe-lean (0.4 wt. % for best carbothermic reduction) and the produced Fe phase Nd-lean (0.1 wt. % for best carbothermic reduction), contaminated only by a reduced fluxing agent (Al) and carbon.
- The CaO- $\text{Al}_2\text{O}_3$ - $\text{Nd}_2\text{O}_3$  phase diagram, obtained via usage of the CALPHAD approach, indicates that the REE content in the slag could be increased to 25 wt. % REE oxides at 1700 °C and even more if small amounts of solid phase still render the slag workable.
- The metallothermic process is preferred because no fossil reduction agent is required, no  $\text{CO}_2$  is emitted and the exothermic heat generation during reduction is increased.
- Leaching of 44 wt. % CaO, 46 wt. %  $\text{Al}_2\text{O}_3$  and 10 wt. %  $\text{Nd}_2\text{O}_3$  in MSA and the addition of NaOH or  $\text{NH}_4\text{OH}$  up to pH 6 resulted in the precipitation of >99% Al, >94% Nd and <1.5% Ca as hydroxides which can be further treated for Nd recovery.
- Slag leaching with  $\text{H}_2\text{SO}_4$  leads to losses of 24% Nd to the gypsum phase and is less promising than the MSA route; nonetheless, the possibility of calcining and recirculating this phase to the 1st step of the pyrometallurgical process (oxidative smelting) exists. Potentially, calcination and oxidative smelting could be integrated in one step.

**Author Contributions:** Conceptualization, L.W.B., D.V. and A.C.; methodology, L.W.B., D.V., A.C. and O.F.; software, O.L. and O.F.; validation, L.W.B., A.A. and O.L.; formal analysis, O.F., O.L. and A.A.; investigation, L.W.B., A.A. and O.L.; resources, A.C. and O.F.; data curation, O.L., A.A., D.V. and



L.W.B.; writing—original draft preparation, L.W.B. and D.V.; writing—review and editing, A.C., D.V., A.A., O.F. and O.L.; visualization, O.L., O.F. and L.W.B.; supervision, A.C.; project administration, L.W.B. and D.V.; funding acquisition, A.C. All authors have read and agreed to the published version of the manuscript.

**Funding:** This research received funding by the EIT RawMaterials funded project DysCOVERY (Sustainable REE, Co supply from magnet recycling: closing the loop), project number 21028.

**Data Availability Statement:** Data will be made available on request.

**Conflicts of Interest:** The authors declare no conflict of interest.

## References

1. Firdaus, M.; Rhamdhani, M.A.; Durandet, Y.; Rankin, W.J.; McGregor, K. Review of High-Temperature Recovery of Rare Earth (Nd/Dy) from Magnet Waste. *J. Sustain. Metall.* **2016**, *2*, 276–295. [CrossRef]
2. Yang, Y.; Walton, A.; Sheridan, R.; Güth, K.; Gauß, R.; Gutfleisch, O.; Buchert, M.; Steenari, B.M.; Van Gerven, T.; Jones, P.T.; et al. REE Recovery from End-of-Life NdFeB Permanent Magnet Scrap: A Critical Review. *J. Sustain. Metall.* **2017**, *3*, 122–149. [CrossRef]
3. Shaw, S.; Constantinides, S. Permanent magnets: The demand for rare earths. In *8th International Rare Earths Conference*; Arnold Magnetic Technologies: Hong Kong, China, 2012; pp. 13–15.
4. Blengini, G.; Latunussa, C.; Eynard, U.; Matos, C.; Georgitzikis, K.; Pavel, C.; Carrara, S.; Mancini, L.; Unguru, M.; Blagoeva, D.; et al. Study on the EU's list of Critical Raw Materials (2020), Final Report. Available online: [https://www.researchgate.net/publication/344124852\\_Study\\_on\\_the\\_EU's\\_list\\_of\\_Critical\\_Raw\\_Materials\\_2020\\_Final\\_Report](https://www.researchgate.net/publication/344124852_Study_on_the_EU's_list_of_Critical_Raw_Materials_2020_Final_Report) (accessed on 28 April 2023).
5. Jadhav, A.P.; Ma, H.; Kim, D.S.; Baek, Y.K.; Choi, C.J.; Kang, Y.S. Nd<sub>2</sub>Fe<sub>14</sub>B Synthesis: Effect of Excess Neodymium on Phase Purity and Magnetic Property. *Bull. Korean Chem. Soc.* **2014**, *35*, 886–890. [CrossRef]
6. Binnemans, K.; Jones, P.T.; Blanpain, B.; Van Gerven, T.; Yang, Y.; Walton, A.; Buchert, M. Recycling of rare earths: A critical review. *J. Clean. Prod.* **2013**, *51*, 1–22. [CrossRef]
7. Takeda, O.; Okabe, T.H. Current Status on Resource and Recycling Technology for Rare Earths. *Metall. Mater. Trans. E* **2014**, *1*, 160–173. [CrossRef]
8. Tanaka, M.; Oki, T.; Koyama, K.; Narita, H.; Oishi, T. Handbook on the Physics and Chemistry of Rare Earths. Elsevier Science Publication: Amsterdam, The Netherlands, 2013; Volume 43, pp. 159–211.
9. Nakamoto, M.; Kubo, K.; Katayama, Y.; Tanaka, T.; Yamamoto, T. Extraction of Rare Earth Elements as Oxides from a Neodymium Magnetic Sludge. *Metall. Mater. Trans. B* **2012**, *43*, 468–476. [CrossRef]
10. Elwert, T.; Goldmann, D.D.; Schirmer, T.; Strauß, K. Affinity of Rare Earth Elements to Silico-Phosphate Phases in the System Al<sub>2</sub>O<sub>3</sub>-CaO-MgO-P<sub>2</sub>O<sub>5</sub>-SiO<sub>2</sub>. *Chem. Ing. Tech.* **2014**, *86*, 840–847. [CrossRef]
11. Bian, Y.Y.; Guo, S.Q.; Xu, Y.L.; Tang, K.; Lu, X.G.; Ding, W.Z. Recovery of rare earth elements from permanent magnet scraps by pyrometallurgical process. *Rare Met.* **2015**, *41*, 1697–1702. [CrossRef]
12. Le, T.H.; Malfliet, A.; Blanpain, B.; Guo, M. Phase Relations of the CaO-SiO<sub>2</sub>-Nd<sub>2</sub>O<sub>3</sub> System and the Implication for Rare Earths Recycling. *Metall. Mater. Trans. B* **2016**, *47*, 1736–1744. [CrossRef]
13. Borra, C.R.; Blanpain, B.; Pontikes, Y.; Binnemans, K.; Van Gerven, T. Smelting of Bauxite Residue (Red Mud) in View of Iron and Selective Rare Earths Recovery. *J. Sustain. Metall.* **2016**, *2*, 28–37. [CrossRef]
14. Kruse, S.; Raulf, K.; Trentmann, A.; Pretz, T.; Friedrich, B. Processing of Grinding Slurries Arising from NdFeB Magnet Production. *Chem. Ing. Tech.* **2015**, *87*, 1589–1598. [CrossRef]
15. Orefice, M.; Van den Bulck, A.; Blanpain, B.; Binnemans, K. Selective Roasting of Nd-Fe-B Permanent Magnets as a Pretreatment Step for Intensified Leaching with an Ionic Liquid. *J. Sustain. Metall. J. Sustain. Metall.* **2019**, *6*, 91–102. [CrossRef]
16. Venkatesan, P.; Sun, Z.H.I.; Sietsma, J.; Yang, Y. Electrochemical recovery of Rare Earth Elements from Magnet scrap-A theoretical analysis. In *ERES2014: 1st European Rare Earth Resources Conference | Milos*. 2014. Available online: [www.researchgate.net](http://www.researchgate.net) (accessed on 28 April 2023).
17. Niskanen, J.; Lahtinen, M.; Peramaki, S. Acetic acid leaching of neodymium magnets and iron separation by simple oxidative precipitation. *Clean. Eng. Technol.* **2022**, *10*, 100544. [CrossRef]
18. Smith, W.R. HSC Chemistry for Windows, 2.0. *J. Chem. Inf. Comput. Sci.* **1996**, *36*, 151–152. [CrossRef]
19. Queneau, P.; Berthold, C. Silica in Hydrometallurgy: An Overview. *Can. Metall. Q.* **1986**, *25*, 201–209. [CrossRef]
20. Lukas, H.L.; Fries, S.G.; Sundmann, B. *Computational Thermodynamics*; Cambridge University Press: Cambridge, UK, 2007.
21. Jantzen, C.M.; Glasser, F.P. Solid-state reactions in the system CaO-Nd<sub>2</sub>O<sub>3</sub>-Fe<sub>2</sub>O<sub>3</sub>-Al<sub>2</sub>O<sub>3</sub>. *Mat Res. Bul.* **1979**, *14*, 1601–1607. [CrossRef]
22. Ilatovskaia, M.; Lonski, O.; Löffler, M.; Blenau, L.; Charitos, A.; Fabrichnaya, O. Phase Relations in the CaO-Nd<sub>2</sub>O<sub>3</sub>-Al<sub>2</sub>O<sub>3</sub> System in Application for Rare Earth Recycling. *JOM* **2023**, *75*, 1993–2002. [CrossRef]
23. Bale, C.W.; Bélisle, E.; Chartrand, P.; Deckerov, S.A.; Eriksson, G.; Gheribi, A.E.; Hack KJung, I.H.; Kang, Y.B.; Melançon, J.; Pelton, A.D.; et al. FactSage Thermochemical Software and Databases—(2010–2016). *Calphad* **2016**, *54*, 35–53. Available online: [www.factsage.com](http://www.factsage.com) (accessed on 28 April 2023). [CrossRef]

24. Jantzen, C.M.; Neurgaonkar, R.R. Solid state reactions in the system  $\text{Nd}_2\text{O}_3\text{-Al}_2\text{O}_3\text{-CaO}$ . *Mat. Res. Bul.* **1981**, *16*, 519–524. [[CrossRef](#)]
25. Andersson, J.O.; Helander, T.; Höglund, L.; Shi, P.F.; Sundmann, B. Thermo-calc & Dictra, computational tools for materials Science. *Calphad Comput. Coupling Phase Diagr. Thermochem.* **2002**, *26*, 273–312.
26. Sarfo, P.; Frasz, T.; Das, A.; Young, C. Hydrometallurgical Recovery and Process Optimization of Rare Earth Fluorides from Recycled Magnets. *Minerals* **2020**, *10*, 340. [[CrossRef](#)]
27. Binnemans, K.; Jones, P.T. Methanesulfonic Acid (MSA) in Hydrometallurgy. *J. Sustain. Metall.* **2023**, *9*, 26–45. [[CrossRef](#)]
28. Voigt, C.; Hubáľková, J.; Zienert, T.; Fankhänel, B.; Stelter, M.; Charitos, A.; Aneziris, C.G. Aluminum Melt Filtration with Carbon Bonded Alumina Filters. *Materials* **2020**, *13*, 3962. [[CrossRef](#)]
29. Zhuchkov, V.I.; Salina, V.A.; Sychev, A.V. The Study of the Process of Metal-Thermal Reduction of Boron from the Slag of the System  $\text{CaO-SiO}_2\text{-MgO-Al}_2\text{O}_3\text{-B}_2\text{O}_3$ . *Sci. Forum* **2019**, *946*, 423–429. [[CrossRef](#)]
30. Gschneidner, K.A.; Calderwood, F.W. The C–Nd (Carbon-Neodymium) system. *Bull. Alloy Phase Diagr.* **1986**, *7*, 557–558. [[CrossRef](#)]
31. Talens Peiró, L.; Villalba Méndez, G. Material and Energy Requirement for Rare Earth Production. *JOM* **2013**, *65*, 1327–1340. [[CrossRef](#)]

**Disclaimer/Publisher’s Note:** The statements, opinions and data contained in all publications are solely those of the individual author(s) and contributor(s) and not of MDPI and/or the editor(s). MDPI and/or the editor(s) disclaim responsibility for any injury to people or property resulting from any ideas, methods, instructions or products referred to in the content.